



## Molecular Crystals and Liquid Crystals

Publication details, including instructions for authors and subscription information:

<http://www.tandfonline.com/loi/gmcl20>

### STRUCTURE AND ELECTRONIC PROPERTIES OF SP<sup>2</sup>/SP<sup>3</sup> MIXED NANO-CARBON SYSTEMS

T. Enoki<sup>a</sup>, B. L. V. Prasad<sup>a</sup>, K. Takai<sup>a</sup> & H. Sato<sup>a</sup>

<sup>a</sup> Department of Chemistry, Tokyo Institute of Technology, Ookayama, Meguro-ku, Tokyo, 152-8551, Japan

Version of record first published: 18 Oct 2010

To cite this article: T. Enoki, B. L. V. Prasad, K. Takai & H. Sato (2002): STRUCTURE AND ELECTRONIC PROPERTIES OF SP<sup>2</sup>/SP<sup>3</sup> MIXED NANO-CARBON SYSTEMS, *Molecular Crystals and Liquid Crystals*, 386:1, 145-149

To link to this article: <http://dx.doi.org/10.1080/10587250215201>

PLEASE SCROLL DOWN FOR ARTICLE

Full terms and conditions of use: <http://www.tandfonline.com/page/terms-and-conditions>

This article may be used for research, teaching, and private study purposes. Any substantial or systematic reproduction, redistribution, reselling, loan, sub-licensing, systematic supply, or distribution in any form to anyone is expressly forbidden.

The publisher does not give any warranty express or implied or make any representation that the contents will be complete or accurate or up to date. The accuracy of any instructions, formulae, and drug doses should be independently verified with primary sources. The publisher shall not be liable for any loss, actions, claims, proceedings, demand, or costs or damages

whatsoever or howsoever caused arising directly or indirectly in connection with or arising out of the use of this material.



## STRUCTURE AND ELECTRONIC PROPERTIES OF $sp^2/sp^3$ MIXED NANO-CARBON SYSTEMS

*T. Enoki, B. L. V. Prasad, K. Takai, and H. Sato*  
*Department of Chemistry, Tokyo Institute of Technology,*  
*Ookayama, Meguro-ku, Tokyo 152-8551, Japan*

*Structures and electronic properties are presented for three types of  $sp^2/sp^3$  mixed nano-carbon systems. Nano-diamond/nano-graphite conversion takes place around 1600°C, which changes the magnetism from  $sp^3$ -defect-dominated one to  $\pi$ -edge state originating one. Fluorination in the initial stage, which prefers edge carbon sites of nano-graphites, destroys the  $\pi$ -edge states, and the succeeding fluorination generates  $sp^3$ -defects with surrounding  $\sigma$ -non-bonding state at the interior carbon sites. Diamond-like-carbon has non-equilibrium  $sp^2/sp^3$  mixed structure with atomic scale disorders, which is easily converted to 3D random network of nano-graphite domains by heat-treatment.*

**Keywords:** disordered carbon; diamond-like carbon; fluorinated graphite; diamond-graphite conversion; nano-graphite

### INTRODUCTION

Since the discoveries of fullerenes and carbon nanotubes, interests in nano-carbon systems have been intensively growing from aspects of mesoscopic physics, supramolecular chemistry and nanotechnology applications. Among these nano-carbon systems, nano-sized diamond and graphene are indispensable partners featured with  $sp^3$  and  $sp^2/\pi$  bonding structures, respectively. In nano-diamond systems, a large contribution of the surface carbon atoms, which lack neighboring carbon atoms in part, makes surface structures modified. In contrast, the edges of a two-dimensional (2D) nano-graphene having open edges are expected to give non-bonding  $\pi$ -electronic state (edge state) of edge origin [1–6]. In this report, we present the structure, electronic and magnetic properties of  $sp^2/sp^3$  mixed nano-carbon systems; nano-diamond/nano-graphite conversion, fluorinated nano-graphite and diamond-like carbons.

The present work was partly supported by the Grant-in-Aid No.13440208 from the Ministry of Education, Science, Sport and Culture, Japan.

## NANO-DIAMOND/NANO-GRAPHITE CONVERSION

Nano-diamond particles with a mean size of 5 nm are converted to nano-sized graphite upon heat-treatment, after removal of functional groups on the surface. As shown in Figure 1, graphitization starts on the surface around 1200°C, extends to the inside around 1400°C, and is finally completed at 1600°C giving nano-graphite particles, which are shaped with polyhedron with a hollow inside and facets composed of stacked 3–6 graphene sheets [3,4]. The electronic and magnetic structures are drastically changed upon the conversion. At low heat-treatment temperatures (HTT) below 1200°C, the electronic structure is described basically in terms of that of diamond, in addition to the presence of  $sp^3$ -defects giving ESR active centers. Graphene sheets with the mean size of 1.5 nm developed on the diamond surface around HTT1200 are not characterized as extended  $\pi$ -electron systems due to the presence of corrugations associated with remaining  $sp^3$  defects, as evidenced by a large  $c$ -axis repeat distance shown in Figure 1. A steep increase in the orbital susceptibility at the expense of localized  $sp^3$ -defect spins above HTT  $\sim$  1400°C is caused by the development of extended  $\pi$ -electronic structure. In nano-graphite produced above HTT  $\sim$  1600°C, there is a large enhancement in the Pauli susceptibility, which is considered to come from the edge states. The orbital susceptibility, which is still smaller than that of bulk graphite, is suggestive of the

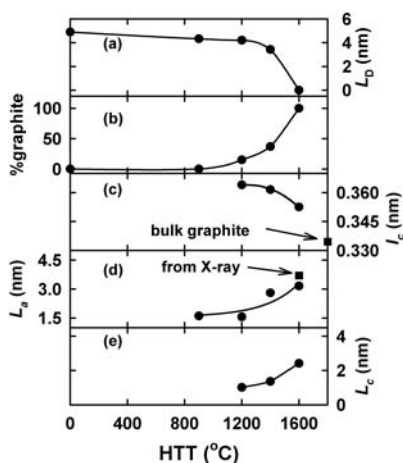


**FIGURE 1** The variation of the structural parameters with HTT in the diamond/graphite conversion. (a) The diamond size ( $L_D$ ), (b) the conversion ratio of diamond to graphite, (c) the observed graphite  $c$ -axis repeat distance ( $I_c$ ), (d) the graphite in-plane domain size ( $L_a$ ), and (e) the graphite thickness along the  $c$ -axis ( $L_c$ ).

presence of edge states in addition to the corrugated feature of graphene sheets.

## FLOURINATED NANO-GRAPHITE

Activated carbon fibers (ACF) are characterized as 3D random network of nano-graphite domains, each of which consists of a stacking of 3–4 graphene sheets with the mean in-plane size of 3 nm. The electronic structure of the nano-graphite is featured with the presence of edge states with localized spins, which gives uniqueness in the magnetic properties of ACFs [5,6]. Fluorination of the nano-graphite works to introduce  $sp^3$  bonds at the carbon atoms, with which fluorine atoms react. Figure 2 shows the F-concentration dependence of localized spin concentration and the orbital susceptibility. The spin concentration monotonically decreases as the  $F/C$  ratio is elevated up to  $F/C \sim 0.4$ , suggesting that edge-state spins successively disappear by the deformation of local structures around the edges due to the fluorination [7]. In that  $F/C$  ratio range, a successive decrease in the orbital susceptibility proves the destruction of the extended  $\pi$ -electronic structure upon fluorination. Above  $F/C \sim 0.4$ , the spin concentration steeply raises with a peak around  $F/C \sim 0.8$ , and then, it decreases followed by the complete elimination of localized spins at  $F/C \sim 1.2$ . The spins generated in that high  $F/C$  range have different magnetic features from those of edge-state spins. The average value of the exchange interaction as a function of  $F/C$  ratio clearly indicates this difference. As shown in Figure 3, the internal magnetic field  $\alpha$ , which has a relatively large value in the pristine ACFs, suggests the presence of

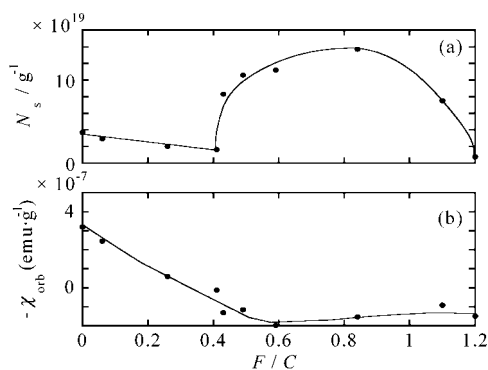


**FIGURE 2** (left) Localized spin concentration  $N_s$  (a), orbital susceptibility  $\chi_{\text{orb}}$  (b) vs  $F/C$  for fluorinated ACFs.

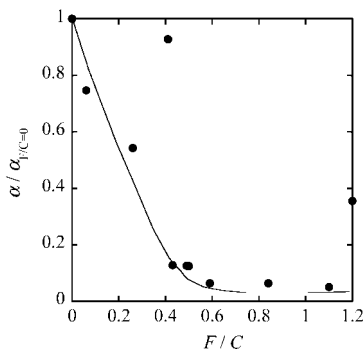


**FIGURE 3** (right) The mean value of the internal field  $\alpha$  vs  $F/C$  ratio in fluorinated ACFs.

exchange interaction between the edge state spins, which is mediated by the conduction  $\pi$ -electrons [6]. The internal field becomes negligible as the  $F/C$  ratio is elevated over  $F/C \sim 0.4$ , suggesting the disappearance of interactions between spins. The spins above that ratio are assigned to  $\sigma$ -dangling bond spins produced at the carbon site neighboring to the carbon site at which a fluorine atom is added in the fluorination. The absence of exchange interaction proves that the  $\sigma$ -dangling bond state has localized feature. The maximum spin concentration is achieved at the  $F/C$  ratio, at which a half of the interior carbon sites react with fluorine atoms, and the completion of  $sp^3$  bonded network at  $F/C \sim 1.2$  sweeps the localized spins away.

## DIAMOND-LIKE CARBONS

Diamond-like carbons with an  $sp^2/sp^3$  ratio of ca.9 were prepared by laser ablation. They do not have any structural regularity according to X-ray diffraction profiles, being suggested to have quenched liquid state in non-equilibrium [8]. The conductivity and thermoelectric power evidence the finite density of states at the Fermi energy, in spite of the absence of extended  $\pi$ -electronic structure. This suggests that liquid carbon featured with a simple  $sp^2/sp^3$  mixture can have extended electronic structure even if it does not have extended  $\pi$ -electronic structure. Heat treatment at considerably low HTT ( $<600^\circ\text{C}$ ) makes the quenched liquid state easily relaxed through the migration of  $sp^3$ -defects, resulting in the formation of  $sp^2$ -dominated nano-graphite-like islands. Figure 4 presents the HTT dependence of the conductivity vs temperature plot. In the low HTT regime below  $1000^\circ\text{C}$ , the conductivity can be explained in terms of variable range

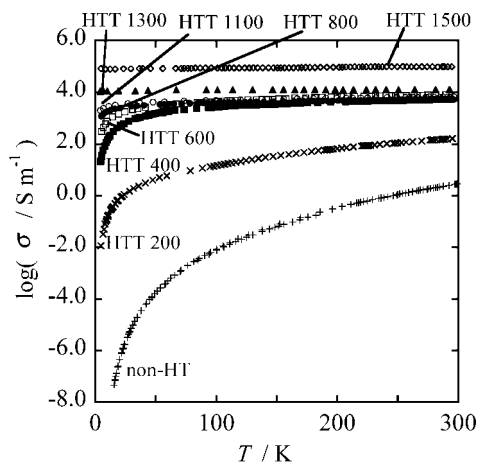


**FIGURE 4** The HTT dependence of the conductivity vs temperature plot in the diamond-like carbon.

hopping in Anderson insulator, where the electron correlation effect is emphasized as HTT is elevated. Around HTT1000, a metal-insulator transition takes place after the development of infinite percolation path network of metallic nano-graphite domains for inter-domain electron transport. The thermoelectric power suggests the presence of inhomogeneous spatial distribution of charges among nano-graphite domains due to the difference of the Fermi levels depending on domains.

## REFERENCES

- [1] Fujita, M., Wakabayashi, K., Nakada, K., & Kusakabe, K. (1996). *J. Phys. Soc. Jpn.*, **65**, 1920.
- [2] Nakata, K., Fujita, M., Dresselhaus, G., & Dresselhaus, M. S. (1996). *Phys. Rev.*, **B54**, 17954.
- [3] Andersson, O. E., Prasad, B. L. V., Sato, H., Enoki, T., Hishiyama, Y., Kaburagi, Y., Yoshikawa, M., & Bandow, S. (1998). *Phys. Rev.*, **B58**, 16387.
- [4] Prasad, B. L. V., Sato, H., Enoki, T., Hishiyama, Y., Kaburagi, Y., Rao, A. M., Eklund, P. C., Oshiyama, K., & Endo, M. (2000). *Phys. Rev.*, **B62**, 11209.
- [5] Shibayama, Y., Sato, H., Enoki, T., Bi, X.-X., Dresselhaus, M. S., & Endo, M. (2000). *J. Phys. Soc. Jpn.*, **69**, 754.
- [6] Shibayama, Y., Sato, H., Enoki, T., & Endo, M. (2000). *Phys. Rev. Lett.*, **84**, 1744.
- [7] Takai, K., Sato, H., Enoki, T., Yoshida, N., Okino, F., Touhara, H., & Endo, M. (2001). *J. Phys. Soc. Jpn.*, **71**, 175.
- [8] Takai, K., Oga, M., Sato, H., Enoki, T., Ohki, Y., Taomoto, A., Suenaga, K., & Iijima, S. submitted to *Phys. Rev.*, **B**.